



DESIGN AND STRUCTURE ACTIVITY RELATIONSHIP (SAR) OF A NOVEL PYRAZINONE SERIES WITH NON-NUCLEOSIDE HIV-1 REVERSE TRANSCRIPTASE INHIBITORY ACTIVITY

Sanjeeva Prasad Tarigopula¹, Manoj Kumar Metta², Philip G.H³, Mounica Sura⁴, Jayasimha Rayalu Daddam^{5*}

^{1,3}Department of Zoology, Sri Krishnadevaraya University, Anantapuramu, A.P, INDIA

²Department of Biotechnology, GIS, GITAM UNIVERSITY, Gandhi Nagar, Rushikonda, Visakhapatnam-530 045, Andhra Pradesh, India

⁴Department of Bioinformatics, Dr.Rayalu's Biotech PVT LTD. Himayath nagar, Hyderabad, Telangana

⁵Department of Biotechnology, Akshaya Biological Corporation, Himayath Nagar, Hyderabad-29. Telangana.

*Corresponding Author Address E-mail: jaimsciotech2007@gmail.com

ABSTRACT: Homology modeling of HIV 1 Reverse Transcriptase has been performed based on the crystal structure of the 2RF2 (Chain A) by using Modeller software. With the aid of the molecular mechanics and molecular dynamics methods, the final model is obtained and is further assessed by procheck and verify 3D graph programs, which showed that the final refined model is reliable. With this model, a flexible docking study HIV 1 Reverse Transcriptase with a group of Pyrazinone series which were selected from the previous publications was performed. The results indicated that MET1, MET3, ARG4, THR5 in HIV 1 Reverse Transcriptase are important determinant residues in binding process as they have strong hydrogen bonding with Pyrazinone series. These hydrogen bonding interactions play an important role for stability of the complex. Among the 12 Pyrazinone series docked, A12 showed best docking result with HIV 1 Reverse Transcriptase. Our results may be helpful for further experimental investigations.

Key words: HIV, Reverse Transcriptase, Homology modelling, Drug designing

INTRODUCTION

Acquired immune deficiency syndrome or acquired immunodeficiency syndrome (AIDS) is a set of symptoms and infections resulting from the damage to the human immune system caused by the human immunodeficiency virus (HIV) [1]. This condition progressively reduces the effectiveness of the immune system and leaves individuals susceptible to opportunistic infections and tumors [2, 3]. HIV is transmitted through direct contact of a mucous membrane or the bloodstream with a bodily fluid containing HIV, such as blood, semen, vaginal fluid, preseminal fluid, and breast milk [4]. Reverse Transcriptase (RT) is a DNA polymerase that will either use an RNA or DNA strand as a primer. It is responsible for the production of a double stranded DNA copy of the single stranded RNA genome that is contained in the HIV-1 virus particle [5,6]. Production of double stranded DNA is primed by the host cell lysine-tRNA which partly unfolds and anneals to the 5' end of the viral genomic RNA [7]. This is extended by the polymerase function of RT to give a DNA-RNA hybrid. The RNA component of this hybrid is degraded by the RNaseH function of RT once it has been copied [8]. The polymerase function of RT is then able to synthesise the second strand of DNA, possibly primed by a rump of the viral RNA. The enzyme reverse transcriptase (RT) is used by retroviruses to transcribe their single-stranded RNA genome into single-stranded DNA and to subsequently construct a complementary strand of DNA, providing a DNA double helix capable of integration into host cell chromosomes [9].

Functional HIV1-RT is a heterodimer containing subunits of 66 kDa (p66) and 51 kDa (p51). p66 contains two domains, the N-terminal polymerase domain (440 residues) and the C-terminal RNase H domain (120 residues). p51 is processed by proteolytic cleavage of p66 and corresponds to the polymerase domain of the p66 subunit.

Portions of both p51 and the polymerase domain of p66 can be described as a "right hand" that contains three subdomains: fingers, palm, and thumb [10]. The connection subdomain connects the hand of the polymerase domain and the RNase H domain in p66, which provides the ribonuclease activity of HIV-RT. Although p51 contains a connection subdomain, it lacks an RNase domain. The connection subdomains and the palm subdomains contain three-stranded beta-sheets with alpha-helices on one side [11]. The thumb subdomains comprise three alpha-helices [12]. Interestingly, although the two subunits are identical in their primary amino acid sequence (except for length), they are structurally very different. This can be clearly seen by observing the subunits separately [13]. Three catalytic residues are exposed in the nucleic acid binding cleft of p66, but are buried in p51, which lacks a discernable cleft. Another striking difference between the two subunits is the orientation of the connection subdomain; in p51 it is tucked into a central position and contacts all of the other subdomains, but in p66 it contacts only RNase H and the thumb. A question arises as to why HIV has evolved a heterodimer in which the smaller subunit (p51) is a cleavage product of the larger. One speculation is that the selection for streamlined genomes in retroviruses has forced the evolution of different protein subunits encoded by the same gene [14]. In the case of HIV-RT, subunits with different structural and functional properties can be produced by proteolytic cleavage of one of two initially identical subunits.

METHODS

3D model building

The initial model of HIV 1 Reverse Transcriptase was built by using homology-modeling methods and the MODELLER software; a program for comparative protein structure modeling optimally satisfying spatial restraints derived from the alignment and expressed as probability density functions (pdfs) for the features restrained. The pdfs restrain $C\alpha$ - $C\alpha$ distances, main-chain N-O distances, main-chain and side-chain dihedral angles. The 3D model of a protein is obtained by optimization of the molecular pdf such that the model violates the input restraints as little as possible. The molecular pdf is derived as a combination of pdfs restraining individual spatial features of the whole molecule. The optimization procedure is a variable target function method that applies the conjugate gradients algorithm to positions of all non-hydrogen atoms. The query sequence from HIV was submitted to domain fishing server for HIV 1 Reverse Transcriptase prediction. The predicted domain was searched to find out the related protein structure to be used as a template by the BLAST (Basic Local Alignment Search Tool) program against PDB (Protein Databank). Sequence that showed maximum identity with high score and less e-value were aligned (Figure 1) and was used as a reference structure to build a 3D model for HIV 1 Reverse Transcriptase. The sequence of HIV 1 Reverse Transcriptase protein (A0MMH7_9HIV1:) was obtained from NCBI. The co-ordinates for the structurally conserved regions (SCRs) for HIV 1 Reverse Transcriptase were assigned from the template using multiple sequence alignment, based on the Needleman-Wunsch algorithm. The structure having the least modeller objective function, obtained from the modeller was improved by molecular dynamics and equilibration methods using NAMD 2.5 software using CHARMM27 force field for lipids and proteins along with the TIP3P model for water (Figure 2B). The energy of the structure was minimized with 1,00,00 steps. A cutoff of 12 Å (switching function starting at 10 Å) for van der Waals interactions was assumed. No periodic boundary conditions were included in this study. An integration time step of 2 fs was used, permitting a multiple time-stepping algorithm to be employed in which interactions involving covalent bonds were computed every time step, short-range nonbonded interactions were computed every two time steps, and long-range electrostatic forces were computed every four time steps. The pair list of the nonbonded interaction was recalculated every ten time steps with a pair list distance of 13.5 Å. The short-range nonbonded interactions were defined as van der Waals and electrostatics interactions between particles within 12 Å. A smoothing function was employed for the van der Waals interactions at a distance of 10 Å. CHARMM27 [force-field parameters were used in all simulations in this study. The equilibrated system was simulated for 1 ps with a 500 kcal/mol/Å² restraint on the protein backbone under 1 atm constant pressure and 310 K constant temperature (NPT) and the Langevin damping coefficient was set to 5 ps unless otherwise stated. Finally, the structure having the least energy with low RMSD (Root Mean Square Deviation) was used for further studies (Figure 2A). In this step, the quality of the initial model was improved. The final structure obtained was analyzed by Ramachandran's map using PROCHECK (Programs to check the Stereo chemical Quality of Protein Structures) and environment profile using ERRAT graph (Structure Evaluation server). This model was used for the identification of active site and for docking of the substrate with the enzyme.

Active site Identification

Active site of HIV 1 Reverse Transcriptase was identified using CASTp server. A new program, CASTp, for automatically locating and measuring protein pockets and cavities, is based on precise computational geometry methods, including alpha shape and discrete flow theory. CASTp identifies and measures pockets and pocket mouth openings, as well as cavities. The program specifies the atoms lining pockets, pocket openings, and buried cavities; the volume and area of pockets and cavities; and the area and circumference of mouth openings.

Docking method

The ligands, including all hydrogen atoms, were built and optimized with chemsketch software suite. Extremely Fast Rigid Exhaustive Docking (FRED) version 2.1 was used for docking studies (OpenEye Scientific Software, Santa Fe, NM). It is an implementation of multiconformer docking, meaning that a conformational search of the ligand is first carried out, and all relevant low-energy conformations are then rigidly placed in the binding site. This two-step process allows only the remaining six rotational and translational degrees of freedom for the rigid conformer to be considered. The FRED process uses a series of shape-based filters and the default scoring function is based on Gaussian shape fitting.

RESULTS AND DISCUSSION

Homology Modeling of HIV 1 Reverse Transcriptase

A high level of sequence identity should guarantee more accurate alignment between the target sequence and template structure. In the results of BLAST search against PDB, only two-reference proteins, including 2RF2 A (Chain A, Crystal Structure and assembly of eukaryotic small heat shock protein) has a high level of sequence identity and the identity of the reference protein with the A0MMH7_9HIV1 domain are 95%. Structurally conserved regions (SCRs) for the model and the template were determined by superimposition of the two structures and multiple sequence alignment.

```

A0MMH7|A0MMH7_9HIV1
PQITLWQRPLVTIKVGGQLKEALLDTGADDTVLEDINLPGKWPKMIGGI 50
gi|164414798|pdb|2RF2|A -----

A0MMH7|A0MMH7_9HIV1
GGFIKVKQYDNICIDICGHKATGTVLVGPTPVNIIGRNLLTQLGCTLNFP 100
gi|164414798|pdb|2RF2|A -----MNSP 4

A0MMH7|A0MMH7_9HIV1
ISPIETVPVKLKP GMDGPKVKQWPLTEEKIKALTEICTEMEKEGKISKIG 150
gi|164414798|pdb|2RF2|A
ISPIETVPVKLKP GMDGPKVKQWPLTEEKIKALVEICTEMEKEGKISKIG 54
*****

A0MMH7|A0MMH7_9HIV1
PENPYNTPVFAIKKKDSTKWRKLVDFRELNKRTQDFWEVQLGIPHPAGLK 200
gi|164414798|pdb|2RF2|A
PENPYNTPVFAIKKKDSTKWRKLVDFRELNKRTQDFWEVQLGIPHPAGLK 104
*****

A0MMH7|A0MMH7_9HIV1
KKKSVTVLDVGDAYFSVPLDKDFRKYTAFTIPSVNNETPGIRYQYNVLPQ 250
gi|164414798|pdb|2RF2|A
KKKSVTVLDVGDAYFSVPLDEDFRKYTAFTIPSINNETPGIRYQYNVLPQ 154
*****

A0MMH7|A0MMH7_9HIV1
GWKGS PAIFQCSMTKILEPFRKQNP DIVIYQYMDDLYVGS DLEIGQHRTK 300
    
```

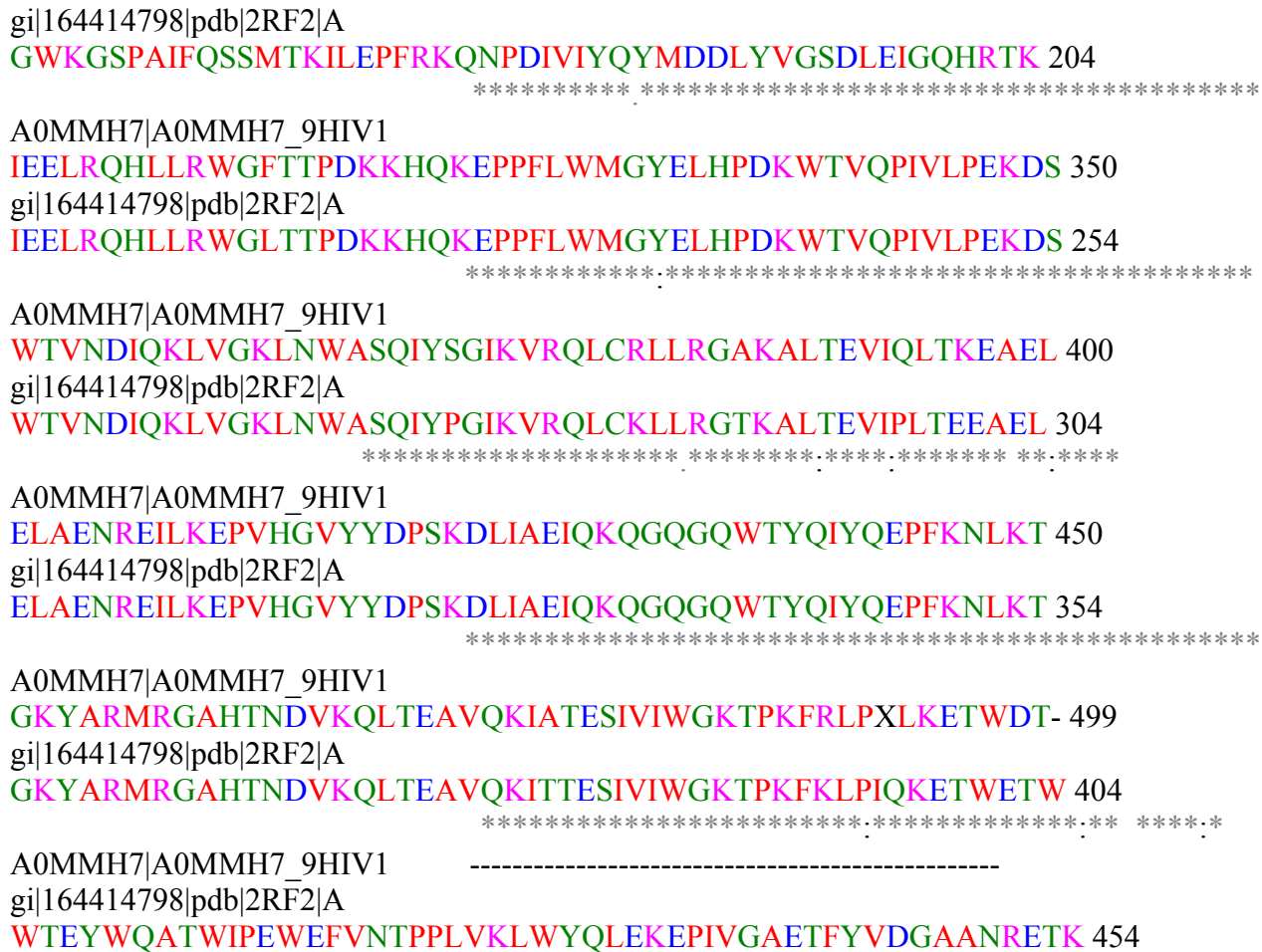


Figure 1: CLUSTAL W multiple sequence alignment

In the following study, we have chosen 2RF2 A as a reference structure for modeling HIV 1 Reverse Transcriptase domain. Coordinates from the reference protein (2RF2 A) to the SCRs, structurally variable regions (SVRs), N-termini and C-termini were assigned to the target sequence based on the satisfaction of spatial restraints. The energy unit will be in kilo joule .All side chains of the model protein were set by rotamers.

The final stable structure of the HIV 1 Reverse Transcriptase protein obtained is shown in Figure 2.

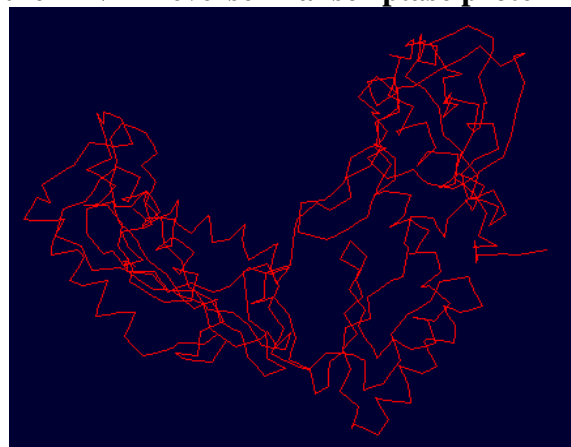


Figure 2: Modelled HIV 1 Reverse Transcriptase

By the help of SPDBV it is evident that HIV 1 Reverse Transcriptase domain has 4 helices and 7 sheets and it is shown in the Figure 3;



Figure 3: Final refined structure of HIV 1 Reverse Transcriptase

The final structure was further checked by verify3D graph and the results have been shown in Figure 4. The overall scores indicates acceptable protein environment.

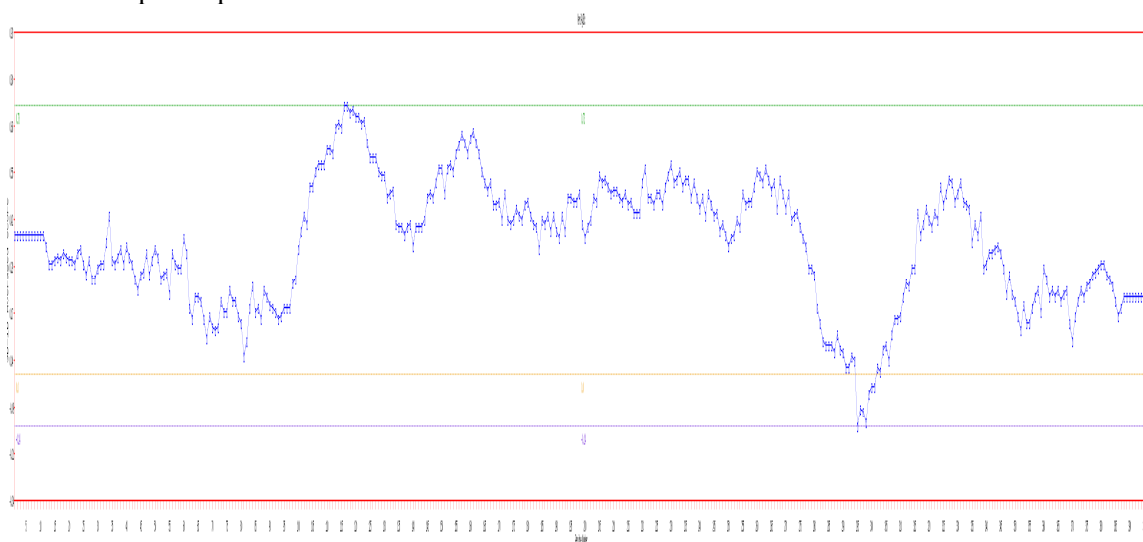


Figure 4: The 3D profiles verified results of HIV 1 Reverse Transcriptase model; overall quality score indicates residues are reasonably folded

Validation of Domain

After the refinement process, validation of the model was carried out using Ramachandran plot calculations computed with the PROCHECK program. The RMSD (Root Mean Square deviation) deviation for covalent bonds and covalent angles relative to the standard dictionary of HIV 1 Reverse Transcriptase was -5.27 and -0.55 Å. Altogether 96.3% of the residues of HIV 1 Reverse Transcriptase was in favored and allowed regions. The overall PROCHECK G-factor of HIV 1 Reverse Transcriptase was -2.32 and verify3D environment profile was good (Fig 5).

Superimposition of 2RF2 A with HIV 1 Reverse Transcriptase domain

The structural superimposition of C trace of template and HIV 1 Reverse Transcriptase is shown in Figure. The weighted root mean square deviation of C α trace between the template and final refined models 0.42 Å. This final refined model was used for the identification of active site and for docking of the substrate with the domain HIV 1 Reverse Transcriptase.

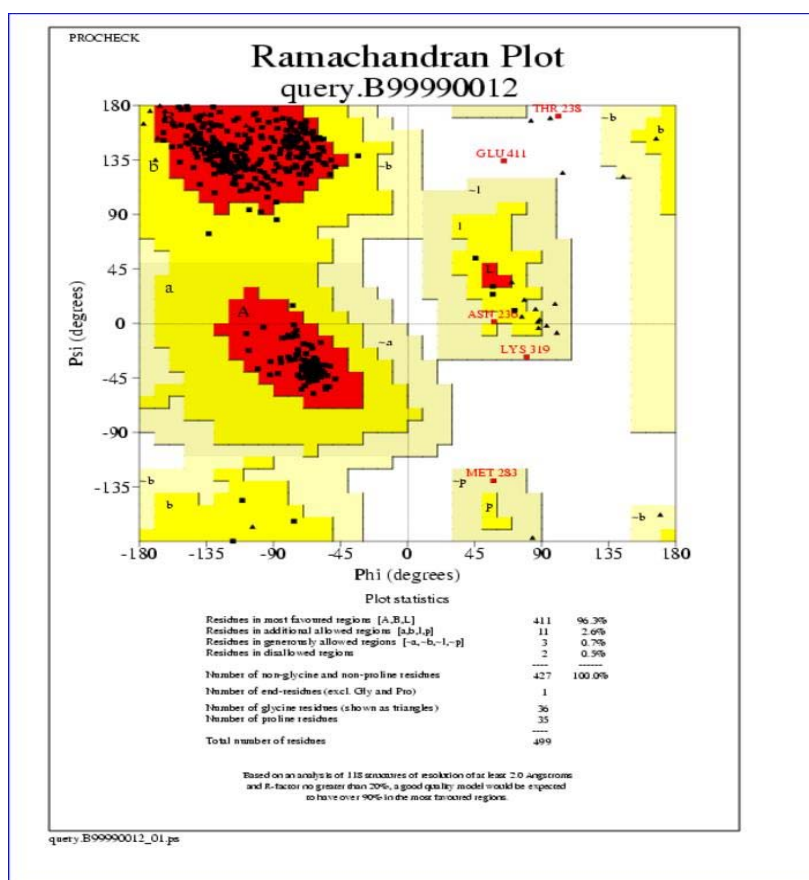


Figure 5: Ramachandran Plot



Figure 6: Superimposition of HIV 1Reverse Transcriptase with 2RF2

Active site Identification of HIV 1 Reverse Transcriptase domain

After the final model was built, the possible binding sites of HIV 1 Reverse Transcriptase was searched based on the structural comparison of template and the model build and also with CASTp server and was shown in Figure 5. Since, HIV 1 Reverse Transcriptase and the 2RF2 A are well conserved in both sequence and structure; their biological function should be identical. Infact from the structure-structure comparison of template, final refined model of HIV 1 Reverse Transcriptase domain using SPDBV program and was shown in Figure3. It was found that secondary structures are highly conserved and the residues.

PHE 99, TRP 123, ILE 136, GLU 139, MET 140, GLU 143, LYS 145, PHE 160, ILE 162, LYS 163, LYS 164, LYS 165, ASP 166, LYS 169, TRP 170, ARG 171, LYS 172, LEU 173, VAL 174, ASP 175, PHE 176, ARG 177, ASN 180, VAL 189, GLN 190, ILE 193, VAL 207, ASP 209, VAL 210, GLY 211, ASP 12, ALA 213, TYR 214, PHE 215, PRO 249, GLN 250, GLY 251, TRP 252, SER 255, PRO 256, PHE 259, GLN 260, MET 263, GLN 281, TYR 282, MET 283, ASP 284, ASP 285, TYR 287, LYS 322, GLU 323, PRO 325, PHE 326, LEU 327, TRP 328, MET 329, GLY 330, GLN 341, PRO 342, ILE 343, VAL 344, ASN 354, LYS 358, GLY 361, LYS 362, TRP 365, LEU 385.

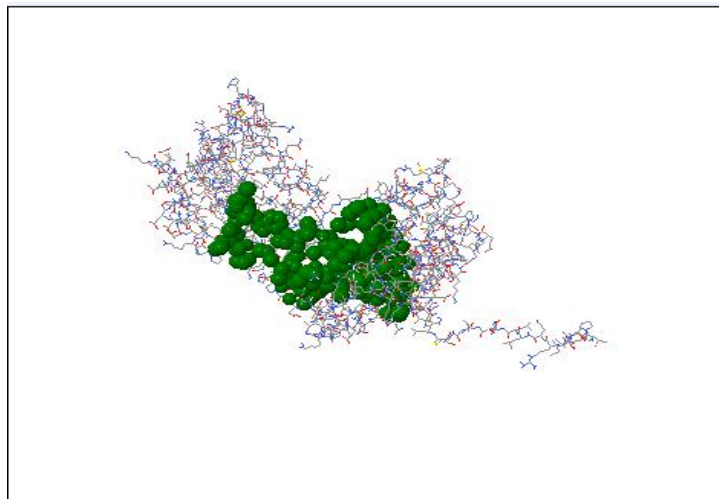
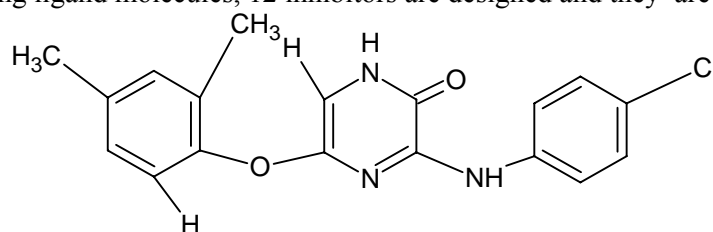


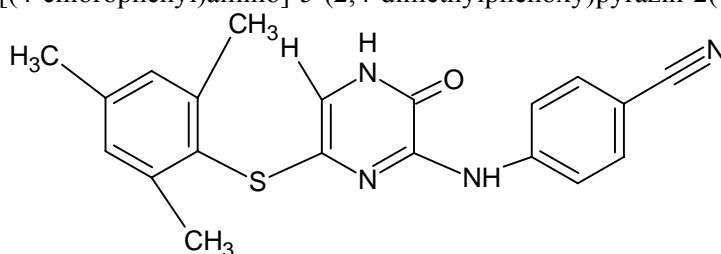
Figure 7: Active site Identification

The Ligand (inhibitor) molecules used for Docking studies

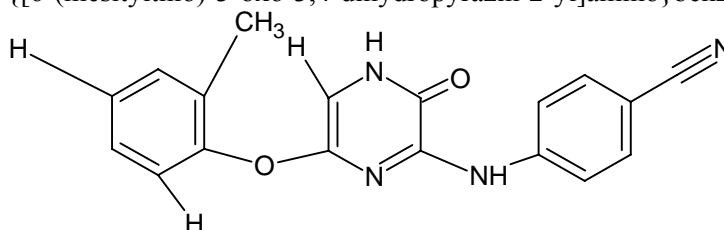
By modifying ligand molecules, 12 inhibitors are designed and they are listed below:



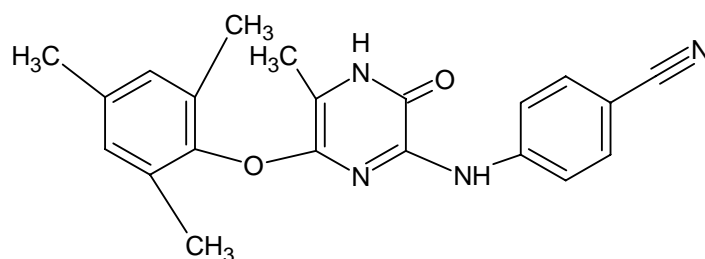
A1. 3-[(4-chlorophenyl)amino]-5-(2,4-dimethylphenoxy)pyrazin-2(1H)-one



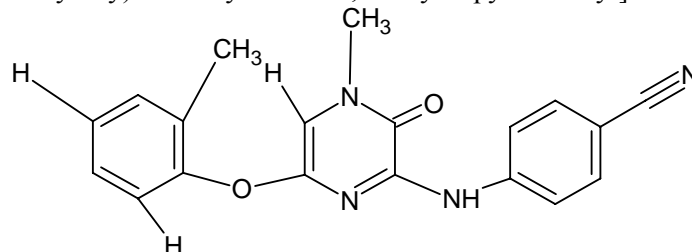
A2. 4-[[6-(mesitylthio)-3-oxo-3,4-dihydropyrazin-2-yl]amino]benzonitrile



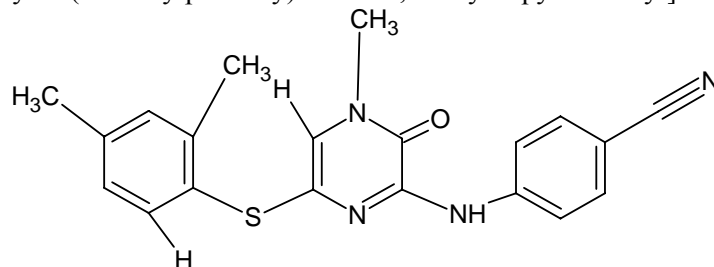
A3. 4-[[6-(2-methylphenoxy)-3-oxo-3,4-dihydropyrazin-2-yl]amino]benzonitrile



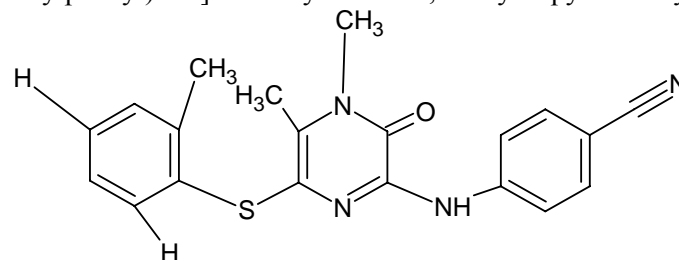
A4. 4-[[6-(mesityloxy)-5-methyl-3-oxo-3,4-dihydropyrazin-2-yl]amino]benzonitrile



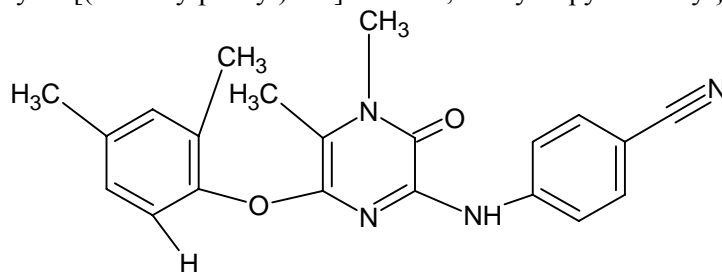
A5. 4-[[4-methyl-6-(2-methylphenoxy)-3-oxo-3,4-dihydropyrazin-2-yl]amino]benzonitrile



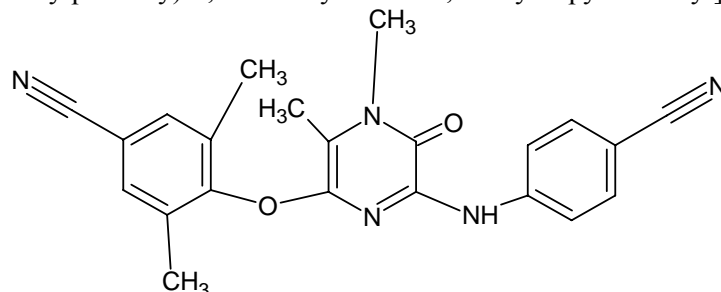
A6. 4-[[6-[(2,4-dimethylphenyl)thio]-4-methyl-3-oxo-3,4-dihydropyrazin-2-yl]amino]benzonitrile



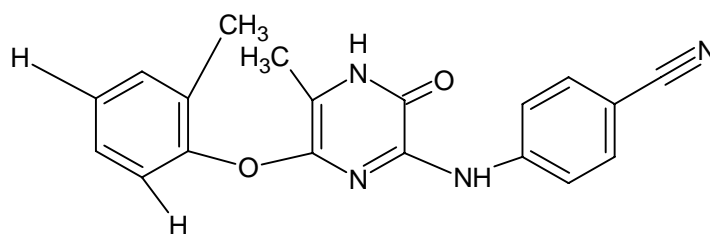
A7. 4-[[4,5-dimethyl-6-[(2-methylphenyl)thio]-3-oxo-3,4-dihydropyrazin-2-yl]amino]benzonitrile



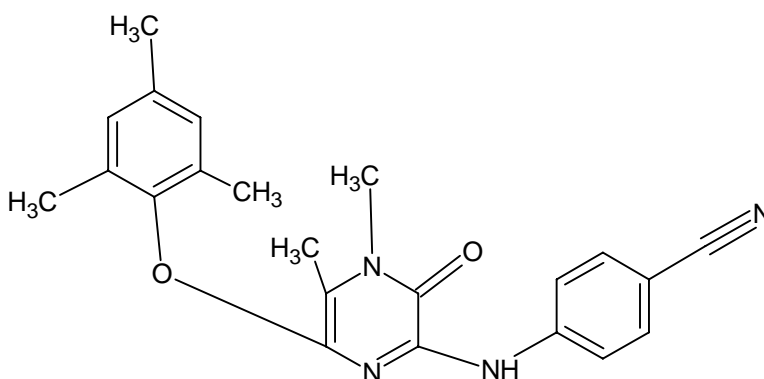
A8. 4-[[6-(2,4-dimethylphenoxy)-4,5-dimethyl-3-oxo-3,4-dihydropyrazin-2-yl]amino]benzonitrile



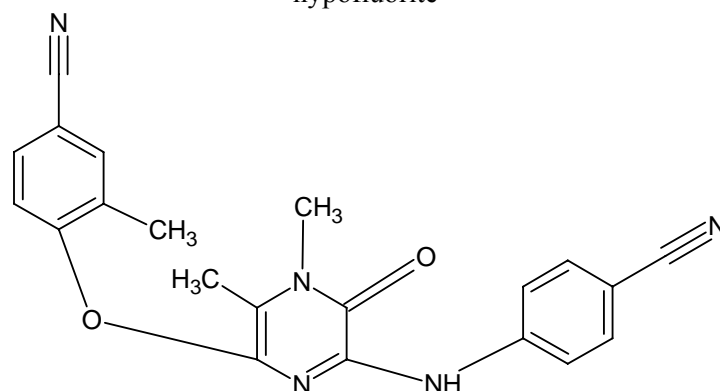
A9. 4-[[6-[(4-cyanophenyl)amino]-3,4-dimethyl-5-oxo-4,5-dihydropyrazin-2-yl]oxy]-3,5-dimethylbenzonitrile



A10. 4-([5-methyl-6-(2-methylphenoxy)-3-oxo-3,4-dihydropyrazin-2-yl]amino)benzonitrile



A11. 4-([6-(mesityloxy)-4,5-dimethyl-3-oxo-3,4-dihydropyrazin-2-yl]amino)benzonitrile hypofluorite



A12. 4-((6-[(4-cyanophenyl)amino]-3,4-dimethyl-5-oxo-4,5-dihydropyrazin-2-yl)oxy)-3-methylbenzonitrile

The Chemical Properties the Structures are tabulated as follows:

Table 1: Chemical properties of the designed derivatives

S.No	Molecular formula	Formula weight	Molar refractivity cm^3	Index of refraction	Density g/cm^3	Polarisability 10^{-24}cm^3
1	$\text{C}_{18}\text{H}_{16}\text{ClN}_3\text{O}_2$	341.79154	93.48 ± 0.5	1.631 ± 0.05	1.30 ± 0.1	37.06 ± 0.5
2	$\text{C}_{20}\text{H}_{18}\text{N}_4\text{OS}$	362.44812	106.25 ± 0.5	1.656 ± 0.05	1.25 ± 0.1	42.12 ± 0.5
3	$\text{C}_{18}\text{H}_{14}\text{N}_4\text{O}_2$	318.32936	90.98 ± 0.5	1.646 ± 0.05	1.27 ± 0.1	36.07 ± 0.5
4	$\text{C}_{21}\text{H}_{20}\text{N}_4\text{O}_2$	360.4091	104.25 ± 0.5	1.621 ± 0.05	1.21 ± 0.1	41.33 ± 0.5
5	$\text{C}_{19}\text{H}_{16}\text{N}_4\text{O}_2$	332.35594	96.31 ± 0.5	1.626 ± 0.05	1.22 ± 0.1	38.18 ± 0.5
6	$\text{C}_{20}\text{H}_{18}\text{N}_4\text{OS}$	362.44812	107.15 ± 0.5	1.646 ± 0.05	1.22 ± 0.1	42.48 ± 0.5
7	$\text{C}_{20}\text{H}_{18}\text{N}_4\text{OS}$	362.44812	107.15 ± 0.5	1.646 ± 0.05	1.22 ± 0.1	42.48 ± 0.5
8	$\text{C}_{21}\text{H}_{20}\text{N}_4\text{O}_2$	360.4091	105.16 ± 0.5	1.612 ± 0.05	1.19 ± 0.1	41.68 ± 0.5
9	$\text{C}_{22}\text{H}_{19}\text{N}_5\text{O}_2$	385.41856	111.68 ± 0.5	1.627 ± 0.05	1.22 ± 0.1	44.27 ± 0.5
10	$\text{C}_{19}\text{H}_{16}\text{N}_4\text{O}_2$	332.35594	95.41 ± 0.5	1.637 ± 0.05	1.25 ± 0.1	37.82 ± 0.5
11	$\text{C}_{22}\text{H}_{22}\text{N}_4\text{O}_2$	374.43568	109.58 ± 0.5	1.606 ± 0.05	1.17 ± 0.1	43.44 ± 0.5
12	$\text{C}_{21}\text{H}_{17}\text{N}_5\text{O}_2$	371.39198	107.26 ± 0.5	1.634 ± 0.05	1.23 ± 0.1	42.52 ± 0.5

Docking of inhibitors with the active site of HIV 1 Reverse Transcriptase:

Docking of the inhibitors given in Figure 6 with HIV 1 Reverse Transcriptase was performed using FRED v 2.1, which is based on Rigid Body Shape-Fitting (Open Eye Scientific Software, Santa Fe, NM). This program generates an ensemble of different rigid body orientations (poses) for each compound conformer within the binding pocket and then passes each molecule against a negative image of the binding site. Poses clashing with this 'bump map' are eliminated. Poses surviving the bump test are then scored and ranked with a Gaussian shape function. We defined the binding pocket using the ligand-free protein structure and a box enclosing the binding site. This box was defined by extending the size of a cocrystallized ligand by 4 Å (addbox parameter of FRED). This dimension was considered here appropriate to allow, for instance, compounds larger than the cocrystallized ones to fit into the binding site. One unique pose for each of the best-scored compounds was saved for the subsequent steps. The compounds used for docking was converted in 3D with OMEGA (same protocol as above) (OpenEye Scientific Software, Santa Fe, NM). To this set, the substrate (generation of multiconformer with Omega) corresponding to the modeled protein were added.

The total energies of Chemguass score, Chemscore, PLP score and shapeguass score of the best-docked conformations of HIV 1 Reverse Transcriptase

Table 2: docking Studies of the Designed Derivatives

Molecule name	Chemgausses	Chemscore	PLP	Screenscore	Shapegausses	TOTAL
1	-45.68	-12.52	-36.79	-84.38	-337.22	-516.59
2	-41.37	-6.93	-34.63	-76.08	-338.53	-497.54
3	-44.65	-12.42	-37.86	-83.04	-325.72	-503.69
4	-47.29	-7.86	-21.54	-62.22	-349.95	-488.86
5	-44.57	-5.76	-34.78	-87.17	-349.63	-521.91
6	-46.84	-4.88	-30.58	-70.54	-346.81	-499.65
7	-39.28	-6.22	-33.97	-68.03	-350.42	-497.92
8	-46.2	-8.68	-35.1	-73.83	-368.12	-531.93
9	-49.58	-6.8	-29.98	-69.51	-375.15	-531.02
10	-42.28	-7.26	-28.26	-67.49	-316.71	-462
11	-43.97	-11.87	-32.32	-63.54	-338.65	-490.35
12	-47.8	-7.79	-38.41	-76.22	-377.19	-547.41

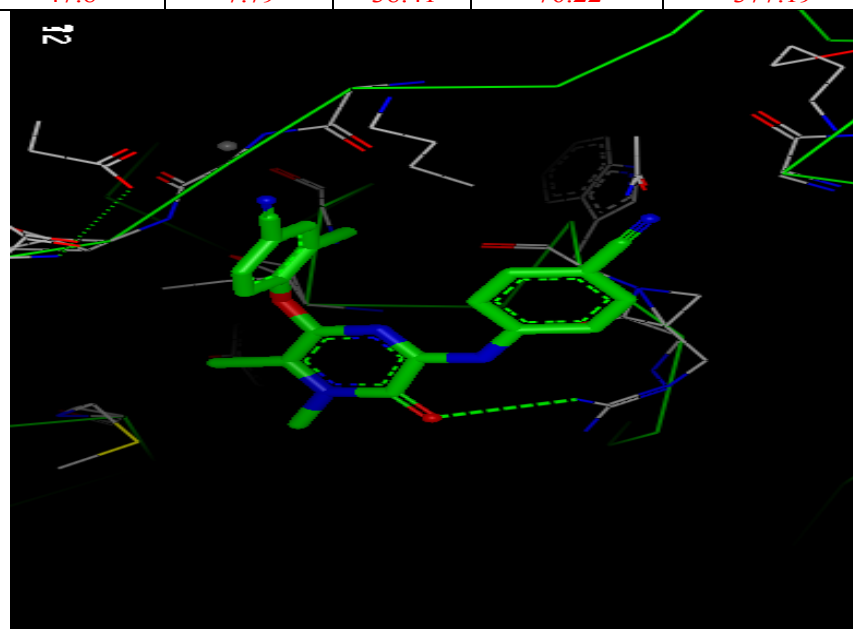


Figure 8: 4-((6-((4-cyanophenyl)amino)-3,4-dimethyl-5-oxo-4,5-dihydropyrazin-2-yl)oxy)-3-methylbenzimidazole docked with HIV-1 Reverse Transcriptase

CONCLUSION

HIV 1 Reverse Transcriptase, is a small heat shock protein. It is a major immune reactive protein in mycobacteria. In this work, we have constructed a 3D model of HIV 1 Reverse Transcriptase domain, using the MODELLER software and obtained a refined model after energy minimization. The final refined model was further assessed by ERRAT and PROCHECK program, and the results show that this model is reliable. The stable structure of HIV 1 Reverse Transcriptase is further used for docking with modified ligand molecules. Docking results indicate that conserved amino-acid residues HIV1 Reverse Transcriptase main play an important role in maintaining a functional conformation and are directly involved in donor substrate binding. The interaction between the domain and the inhibitors proposed in this study are useful for understanding the potential mechanism of domain and the inhibitor binding. As is well known, hydrogen bonds play important role for the structure and function of biological molecules. In this study it was found that, PHE 99, TRP 123, ILE 136, GLU 139, MET 140, GLU 143, LYS 145, PHE 160, ILE 162, LYS 163, LYS 164, LYS 165, ASP 166, LYS 169, TRP 170, ARG 171, LYS 172, LEU 173, VAL 174, ASP 175, PHE 176, ARG 177, ASN 180, VAL 189, GLN 190, ILE 193, VAL 207, ASP 209, VAL 210, GLY 211, ASP 212, ALA 213, TYR 214, PHE 215, PRO 249, GLN 250, GLY 251, TRP 252, SER 255, PRO 256, PHE 259, GLN 260, MET 263, GLN 281, TYR 282, MET 283, ASP 284, ASP 285, TYR 287, LYS 322, GLU 323, PRO 325, PHE 326, LEU 327, TRP 328, MET 329, GLY 330, GLN 341, PRO 342, ILE 343, VAL 344, ASN 354, LYS 358, GLY 361, LYS 362, TRP 365, LEU 385 are important for strong hydrogen bonding interaction with the inhibitors. To the best of our knowledge MET1, MET3, ARG4, THR5 are conserved in this domain and may be important for structural integrity or maintaining the hydrophobicity of the inhibitor-binding pocket. The molecule A12 showed best docking results with target protein.

REFERENCES

- [1] Weiss RA. 1993. "How does HIV cause AIDS?". *Science (journal)* 260 (5112): 1273–9.
- [2] Divisions of HIV/AIDS Prevention (2003). "HIV and Its Transmission". Centers for Disease Control & Prevention. Retrieved on 2006-05-23.
- [3] San Francisco AIDS Foundation 2006. "How HIV is spread". Retrieved on 2006-05-23.
- [4] Kallings LO 2008. "The first postmodern pandemic: 25 years of HIV/AIDS". *J Intern Med* 263 (3): 218–43.
- [5] UNAIDS, WHO (December 2007). "2007 AIDS epidemic update" (PDF). Retrieved on 2008-03-12.
- [6] Bell C, Devarajan S, Gersbach H. "The long-run economic costs of AIDS: theory and an application to South Africa" (PDF). World Bank Policy Research Working Paper No. 3152. Retrieved on 2008-04-28.
- [7] Gao F, Bailes E, Robertson DL. 1999. "Origin of HIV-1 in the Chimpanzee Pan troglodytes troglodytes". *Nature* 397 (6718): 436–441.
- [8] Gallo RC 2006. "A reflection on HIV/AIDS research after 25 years". *Retrovirology* 3: 72.
- [9] Palella FJ Jr, Delaney KM, Moorman AC. 1998. "Declining morbidity and mortality among patients with advanced human immunodeficiency virus infection. HIV Outpatient Study Investigators". *N. Engl. J. Med* 338 (13): 853–860.
- [10] Holmes CB, Losina E, Walensky RP, Yazdanpanah Y, Freedberg KA 2003. "Review of human immunodeficiency virus type 1-related opportunistic infections in sub-Saharan Africa". *Clin. Infect. Dis.* 36 (5): 656–662.
- [11] Guss DA 1994. "The acquired immune deficiency syndrome: an overview for the emergency physician, Part 1". *J. Emerg. Med.* 12 (3): 375–384.
- [12] Guss DA 1994. "The acquired immune deficiency syndrome: an overview for the emergency physician, Part 2". *J. Emerg. Med.* 12 (4): 491–497.
- [13] Feldman C 2005. "Pneumonia associated with HIV infection". *Curr. Opin. Infect. Dis.* 18 (2): 165–170.
- [14] Decker CF, Lazarus A. 2000. "Tuberculosis and HIV infection. How to safely treat both disorders concurrently". *Postgrad Med.* 108 (2): 57–60, 65–68.

International Journal of Plant, Animal and Environmental Sciences

